



Available online at [www.sciencedirect.com](http://www.sciencedirect.com)

**ScienceDirect**

Energy Procedia 85 (2016) 260 – 265

Energy

**Procedia**

Sustainable Solutions for Energy and Environment, EENVIRO - YRC 2015, 18-20 November  
2015, Bucharest, Romania

## Numerical study for open-channel flow over rows of hemispheres

Elena Iatan<sup>a\*</sup>, Marius Iliescu<sup>a</sup>, Florin Bode<sup>b\*</sup>, Ilinca Nastase<sup>a</sup>,  
Radu Mircea Damian<sup>a</sup>, Mihnea Sandu<sup>a</sup>

<sup>a</sup>*Technical University of Civil Engineering in Bucharest, Building Services Department, 66 Avenue Pache Protopopescu;  
020396, Bucharest, Romania*

<sup>b</sup>*Technical University of Cluj-Napoca, Cluj-Napoca, Romania*

---

### Abstract

Important parameters in the study of design criteria for sewer pipes are related to shear velocity. The aim of this paper is to obtain a numerical model which does not require significant computational resources and that is feasible for the calculation of shear velocity. We created a numerical model in a free surface flow over artificial roughness elements represented by hemispheres. The numerical model is designed to be identical with an experimental model previously studied. We have investigated velocity and vorticity fields and the distribution of turbulent stresses using a SST  $k - \omega$  model.

© 2016 Published by Elsevier Ltd. This is an open access article under the CC BY-NC-ND license

(<http://creativecommons.org/licenses/by-nc-nd/4.0/>).

Peer-review under responsibility of the organizing committee EENVIRO 2015

**Keywords:** Artificial roughness; hemispheres;  $k-\omega$  SST model; particle image velocimetry

---

### 1. Introduction

It is of practical interest to understand and evaluate the effects that the presence of additional roughness will generate in the water flowing in a sewer pipe. Various experimental and numerical studies were performed to investigate flow characteristics of artificially roughened channels. In this study the additional roughness is represented by periodic rows of hemispheres with the length-to depth ratio equal to 4. The water flowing in this channel is numerically investigated using  $k-\omega$  shear stress transport ( $k-\omega$  SST) turbulence model, on a three-dimensional (3-D) domain.

---

\* Corresponding author.

E-mail address: [eserban@instal.utcb.ro](mailto:eserban@instal.utcb.ro); [florin.bode@termo.utcluj.ro](mailto:florin.bode@termo.utcluj.ro)

An important method used for the study of flows over different roughness elements is the Computational Fluid Dynamics method (CFD). The flow field is completely described by Navier–Stokes equations that are non-linear partial differential equations. Direct Numerical Simulation (DNS) and Large Eddy Simulation (LES) are used for numerically solving Navier–Stokes equations, providing the most accurate solutions. Comparative results between DNS and LES are found in literature and in some circumstances LES is performing almost “like DNS”, see [1]. D. Chatzikiyriakou et al. (2015) performed a DNS vs LES comparative study and determined that in LES simulations the values of turbulent kinetic energy is equal to at least 94% of the values of the kinetic energy computed in the DNS simulation [2]. The disadvantage of these two techniques (DNS and LES) is that they are requiring significant computational resources.

Most of the numerical studies of the fluid flow over roughness elements use the Reynolds-Averaged Navier–Stokes (RANS) method with different turbulence models. RANS models, although they are introducing numerical and physical approximations, can perform reasonably accurate with less computational resources. Numerous studies for different wall-mounted obstacles have been performed by using turbulence models like standard  $k-\epsilon$  model, modified  $k-\epsilon$  model, Reynolds Stress Model, DNS and LES. Previous studies [3] have shown that  $k-\epsilon$  RANS models can have problems in simulating the details of the flow over arrays of cubes. In particular they can overestimate turbulence energy upstream of stagnation points and do not capture accurately separation and reattachment processes. On the other hand, more accurate LES simulations can reproduce such details of the flow, having the disadvantage of a more expensive time calculation (e.g. Cheng et al. 2003).

Xie and Castro (2006) performed a numerical study including a comparison between LES and RANS emphasizing that the latter is inadequate, especially within the canopy region. The proposed RANS models in their study (SKE, MKE, RSM) underestimate the stream-wise mean velocity within the canopy and both the SKE and MKE models fail to predict a reverse flow on the lateral sides of the cube. All the RANS models underestimate the TKE in the canopy, when compared with the LES results. As a general conclusion SKE performed the worst.

Peng et al. (2011) studied the thermal/hydraulic performance of different ribs, also in terms of Nusselt number and friction factor, with the shear-stress transport model,  $k-\omega$  SST. The numerical results for friction factor are observed to be much larger than the experimental data. A good agreement between numerical and experimental results is observed for the variation of the Nusselt number.

Tang and Zhu (2013) investigated the turbulent flow and heat transfer in a rectangular channel with inclined broken ribs. Numerical results are evaluated by comparison with experimental data for Nusselt number and friction factor and they concluded that the  $k-\omega$  SST model is more suitable than RNG  $k-\epsilon$  model for numerical simulation of flow and heat transfer in ribbed channels. Differences between experimental and numerical results for Nusselt number and friction factor are less than 10% and 7% respectively.

The main objective of the present study is to investigate and determine the range within which the numerical  $k-\omega$  SST model responds correctly, compared to the experimental data, for the geometry presented in Fig. 1. The authors investigated velocity fields and the Reynolds stress distribution. Shear velocity is a critical element in the studies concerning flows over rough surfaces and can be calculated from the velocity distributions or Reynolds stresses. The procedures are not presented in this paper, for references see [6], [7], [8].

## 2. Experimental measurements

The experiments were performed in a closed loop water system of pipes. A short geometrical description is presented in Fig. 1 and considers a three-dimensional free surface flow of water over wall-mounted hemispheres at the bottom wall of the channel.

The channel is circular with a diameter of 14 cm. The water depth  $H$  is equal to 68 mm. The diameter of the hemispheres  $\Phi$  is 4,5 mm and the height of the hemisphere  $h$  is 2,25mm. The water depth is corresponding to 27 times the hemisphere height ( $H/h=68/2,25=30$ ). The section in which the measurements were made is positioned at 3,5m from the water inlet and it includes three consecutive hemispheres (in the flow direction) along the row R3 (see Fig. 1). The rows are made of calibrated hemispheres attached to the bottom model surface.

The flow rates in the supply pressure pipe were measured by a volumetric flow meter with accuracy of 3%. The measured water temperature was  $22^{\circ}\text{C} \pm 10\text{C}$ , for which the corresponding kinematic viscosity was taken  $0,93 \text{ (m}^2/\text{s)} \times 10^{-6}$ . The bulk Reynolds number of the flowing water, based on the hydraulic radius, was 16,000.

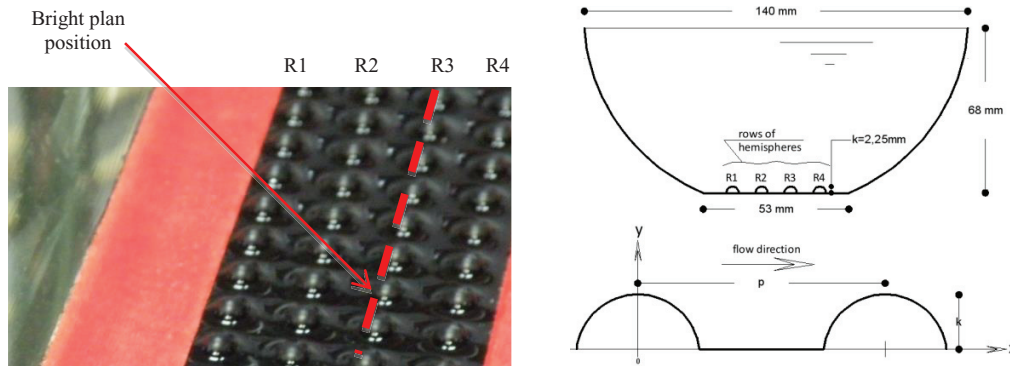


Fig. 1. Measuring section (figure left) and geometry of the problem (figure right): 68 mm is the depth of the free surface flow, p is the length between two hemispheres, k is half the diameter of the hemispheres,  $p/k = 4$ . Flow direction is along the measuring section.

Measurement PIV campaigns was carried out using a Dantec system composed of a high sensitivity camera FlowSense MKII 4M having a resolution of  $4 * 10^6$  pixels and a laser Litronic 200mJ that produces a bright plan with a wavelength 532nm. The acquisition system frequency is 7.5Hz. Calibration images resulted in a spatial resolution of  $11.5 \times 10^{-3}$  mm / pixel corresponding to a field of view  $23\text{mm} \times 23\text{mm}$ . A total of 300 pairs of images is obtained and transformed using a correlation algorithm multilevel grid view of deformation and displacement sub-pixel cells. The final grid cell is composed of  $16 \times 16$  pixeli<sup>2</sup> with 50% coverage which can be translated as a vector to every 127 pixels or a spatial resolution of 0.18 mm.

On average, less than 5% of the vectors were found to be invalid. They were corrected by a bilinear interpolation. A systematic inspection of travel histograms show a bimodal distribution well discretized.

### 3. Field computation

The calculations were performed for a domain that reproduced the geometrical and experimental flow conditions. In the experimental set-up, the flow is confined by a plexiglas pipe having the geometrical dimensions described in paragraph 2.

The grid for the computations consisted of 2,73 million elements computational cells. Fig. 3 shows non-uniform unstructured grid details. For the geometrical discretization we used polyhedral cells because these are producing equivalent accuracy results compared to other mesh types, a faster convergence and robust convergence to lower residual values than other mesh types and therefore this will lead to faster solution runtimes. A grid independence test was carried out, for which we have generated three different polyhedral meshes: 1,3, 2,73 and 3,45 million of polyhedrons (see Fig. 3) were generated. The results obtained with the 2,73 and 3,45 million elements, in terms of velocity profiles, were similar with the results obtained by PIV technique, therefore for the following studies we choose the 2,73 million of tetrahedron elements.

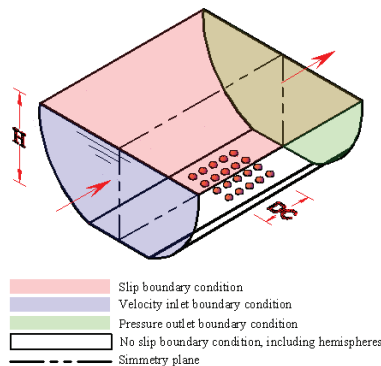


Fig. 2. Discretization domain (DC) with boundary conditions. Flow direction is from left to right.

Turbulent flows are significantly affected by the presence of walls. Mean velocity is affected by the no-slip condition and the wall is also the main sources of turbulence production. Very close to the wall viscosity cancels velocity fluctuations but in the near-wall region, toward the outer layer, the turbulence develops rapidly by the production of turbulence kinetic energy due to the large gradients in mean velocity. The result of the mechanisms described above is that near-wall modelling has a very significant impact on the accuracy of the numerical solutions.

The first grid point from the wall was positioned in the linear region to ensure that non-dimensional wall distance  $y^+$  was less than 1.0 [Fluent Inc., Fluent 6.3 User's Guide, 2003].

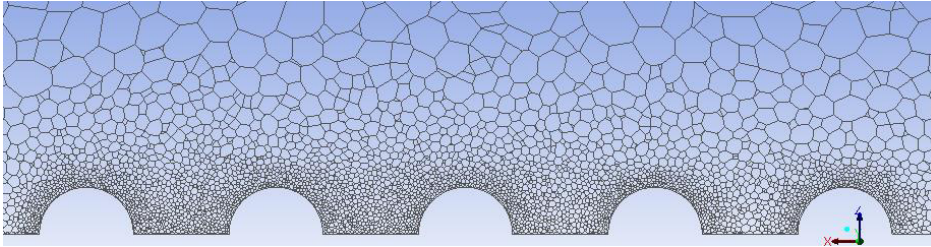


Fig. 3. Discretization domain along the row R3 in the flow direction for 2,73 million of tetrahedrons. Five consecutive hemispheres are included in every row.

#### 4. Numerical results, SST $k - \omega$ Model

The  $k - \omega$  SST model is a combination of a  $k - \omega$  model (in the inner boundary layer) and a  $k - \epsilon$  model (in the outer region of the boundary layer as well as outside of it) [3]. The  $k - \omega$  model is well suited for prediction in the vicinity of the wall, while the  $k - \epsilon$  model is used for the remaining area near the boundary region. The  $k - \omega$  SST model is known to be fairly effective for evaluations of flow separation.

The mathematical model is not presented in this work. For a detailed description of the model see [9] and Fluent User Guide.

Commercial computational fluid dynamics (CFD) software, FLUENT 6.3.26. was used to solve the model equations.

The numerical model validation is performed by comparison of computed velocity fields and velocity profiles obtained from experimental results see Fig. 4 and Fig. 5. The recirculation is observed in the middle of the cavity created between two hemispheres, which corresponds to literature data for roughness with  $p/k = 4,5$  see [4] for water flowing over ribs of hemispheres and see [5] for open channel flow over bars with sharp edges. Numerical model captures this recirculation phenomenon.

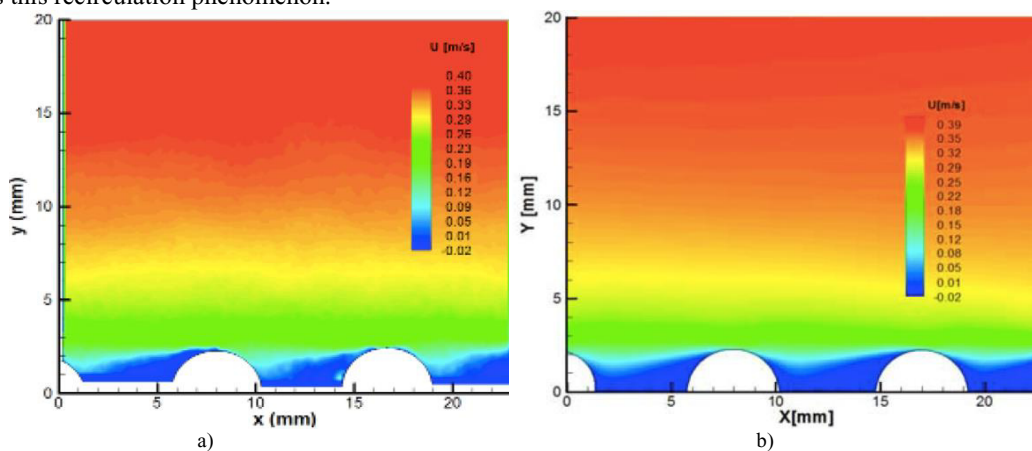


Fig. 4. Velocity field a) from PIV experiment and b) from numerical model.

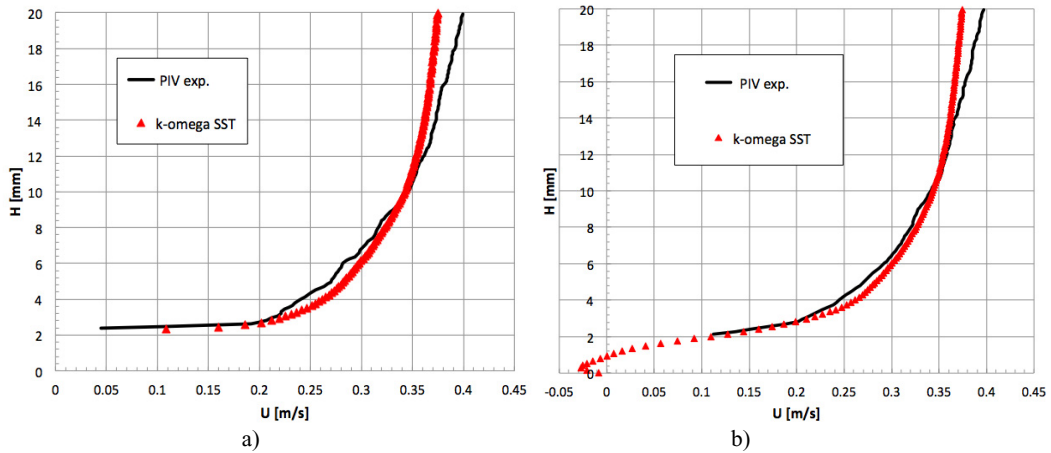


Fig. 5. Velocity profiles at a) a vertical line in the centre of the hemisphere and b) a vertical line in the centre of the cavity between two consecutive hemispheres.

After reaching a minimal value, the velocity growth over the depth of the flow is almost linear. We observe a good correlation between experimental and computed velocity profiles for both positions. In Fig. 6 we present the comparison between experimental and numerical obtained for transversal vorticity. The presented domain is a longitudinal plane in the middle of row 3 with 2 centimetres from the entire depth of the flow. As can be seen areas associated with negative vorticity (blue fields) of the normal vortex generated by hemispheres are captured accurately right.

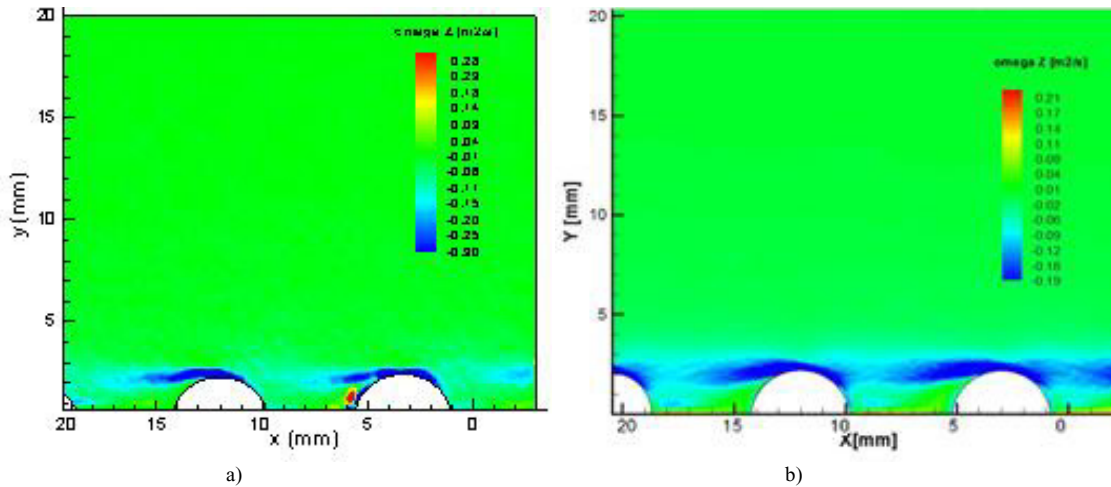


Fig. 6. Transversal vorticity a) from PIV experiment and b) from numerical model. Flow is from right to left.

In Fig. 6 Reynolds stress distribution is represented using a SST  $k-\omega$  model. A maximum value of stress can be noted at about 43% from the depth of the flow. In the literature experimental results presents a maximum at around 20% - 30% from the depth of the flow [6], at around 10% - 15% from the depth of the flow. We conclude that in our case the maximum position is shifted upwards. Typically Reynolds stress profiles follow a linear distribution above the maximum that can be observed in our numerical results.

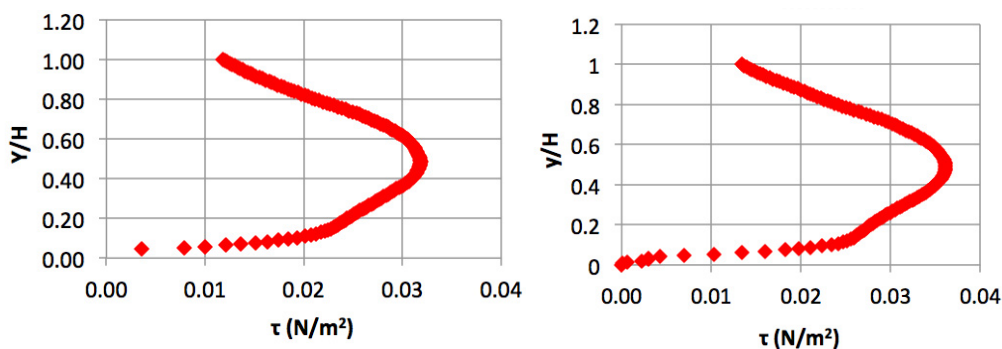


Fig. 6. Reynolds stress distribution from numerical model for: a) a vertical profile in the centre of the hemisphere and b) a vertical profile in the centre of the cavity between two consecutive hemispheres. Flow is from left to right.

## 5. Conclusions

We performed a numerical simulation of a flow over rows of hemispheres using a  $k-\omega$  SST model. The numerical model that was carried out in this article is designed to be identical with an experimentally previously investigated model. The aim of the numerical simulation was to determine the range within which the numerical  $k-\omega$  SST model responds correctly, compared to the experimental data, for the considered geometry. We identified a good correlation between experimental and numerical velocity profiles.

Reynolds stresses presents the maximum position shifted upwards by comparison with experimental data we found in the literature. We conclude that this numerical model can be applied to calculate shear velocity through methods using velocity distributions. However, the results obtained using the method based on turbulent stresses distribution are less precise.

## References

- [1] Zhengtong Xie, Ian P. Castro, LES and RANS for turbulent flow over arrays of wall-mounted obstacles, *Flow Turbulence Combust* (2006) 76:291–312.
- [2] D. Chatzikyriakou, J. Buongiorno, D. Caviezel, D. Lakehal, DNS and LES of turbulent flow in a closed channel featuring a pattern of hemispherical roughness elements, *International Journal of Heat and Fluid Flow*, Volume 53, June 2015, Pages 29–43.
- [3] Lars Davidson, Fluid mechanics, turbulent flow and turbulence modeling, [http://www.tfd.chalmers.se/~lada/MoF/lecture\\_notes.html](http://www.tfd.chalmers.se/~lada/MoF/lecture_notes.html)
- [4] Martin Agelinchab, Mark F. Tachie, Open channel turbulent flow over hemispherical ribs, 2006, *International Journal of Heat and Fluid Flow* 27 1010-1027, Elsevier.
- [5] Thorsten Stoesser, Vladimir I. Nikora, Flow structure over square bars at intermediate submergence: Large Eddy Simulation study of bar spacing effect, *Acta Geophysica*, vol. 56, no. 3, pp. 876-893.
- [6] Fereshteh Bagherimiyab, Ulrich Lemmin, Shear velocity estimates in rough-bed open channel flow, *Earth Surf. Process. Landforms* 38, 1714–1724 (2013), John Wiley & Sons, Ltd., Published online 16 April 2013 in Wiley Online Library.
- [7] Pascale M. Biron, Colleen Robson, Michel F. Lapointe, Susan J. Gaskin, Comparing different methods of bed shear stress estimates in simple and complex flow fields. *Earth Surf. Process. Landforms* 29, 1403–1415, 2004.
- [8] Pawel M. Rowinski, Jochen Aberle, Agata Mazurczyk, Shear velocity estimation in hydraulic research, *Acta Geophysica Polonica*, Vol. 53, No. 4, pp. 567-583, 2005
- [9] Florian R. Menter, Review of the shear-stress transport turbulence model experience from an industrial perspective,